Electrophotographic Process in a High Speed Printer

Abstract: The IBM 3800 printing subsystem was developed for on-line computer system output printing in hard copy form at high speeds. The subsystem combines laser and electrophotographic technology with a multiformat paper handling system and on-line character set variability to provide increased data handling flexibility, throughput and print quality at reduced cost. This paper presents design considerations for the electrophotographic process. It provides an overview of the process and discusses methods and technical approaches used in the design of the printer.

Introduction

Although the data handling ability of computer systems has greatly increased during the last decade, the improvements in output printing have been rather modest. In some instances the printer became a bottleneck in data processing installations.

The basic design consideration for a new printing system, therefore, was to speed up the on-line operation. Because mechanical impact printers appeared to have reached their speed and reliability limitations, various nonimpact printing technologies were considered. Among the options, only the electrophotographic process had been developed to a point where an application in a high speed on-line printer, with its inherent requirements for data integrity and reliability, appeared feasible for an output device which should be compatible with the plain paper media used in conventional impact print installations.

The selection of a nonimpact technology created the desired effect of increased flexibility of printing with multiset characters, and, in addition, provided a means for generating standard forms while simultaneously printing on-line data. Paper format and paper handling components had to meet the requirements of the same market as conventional impact printers while simultaneously reducing the paper handling operations that would be required before and after printing.

These design objectives have been realized in the IBM 3800 printing subsystem, which is based on electrophotographic and laser technologies in combination with high speed paper handling and control systems. This paper concentrates on the electrophotographic printing process. Complementary papers in this issue discuss the design of the paperline [1], the control unit [2], the paper servo [3], and the fuser [4].

The printing process has been designed to operate with a continuous fanfold paperline at a paper speed of 80 cm/s. This is equivalent to a printing speed of approximately 10 020 lines per minute at a conventional print density of six lines per inch. The process speed is independent of line density, so that at the increased line densities of eight and twelve lines per inch, the equivalent printing speed would be 13 360 and 20 040 lines per minute respectively.

The printer process is schematically shown in Fig. 1. The application of the electrophotographic process to high speed printing required a specific choice of components, as well as redesign of certain components to produce quality print and impart sufficient reliability to the printing subsystem. The two exposure units, laser and forms flash, were designed specifically for the printer application. The charge corona, the developer, and the photoconductor restoration units were redesigned to meet the high speed requirements of the electrophotographic process. The design of the transfer unit allowed fast stops and starts of the paperline and utilization of a variety of papers normally used in computer output printing. The fuser system was designed to reliably handle high speed paper. To retain the print quality over variable print demand, a closed loop print density control

Copyright 1978 by International Business Machines Corporation. Copying is permitted without payment of royalty provided that (1) each reproduction is done without alteration and (2) the *Journal* reference and IBM copyright notice are included on the first page. The title and abstract may be used without further permission in computer-based and other information-service systems. Permission to *republish* other excerpts should be obtained from the Editor.

was incorporated in the high speed printer through an optical print mark sense unit.

Photoconductor charging and discharging

The electrophotographic process was developed around an organic photoconductor used in the IBM Copiers I and II. The physical properties of the organic photoconductor, a charge transfer complex of poly-N-vinylcarbazole and 2,4,7-trinitro-9-fluorenone, have been published in detail by Schaffert [5]. The photoconductor in the form of a flexible film is wrapped around a drum, which rotates at a constant surface speed. The photoconductor can be renewed after use by advancing a fresh portion of the film from a supply reel (Fig. 1). The photoconductor is charged to a negative potential of about -750 V by means of a high-voltage charge corona device. The charged photoconductor is subsequently exposed to a potential of about -200 V, to provide a contrast potential of about 550 V between exposed and unexposed areas. Two exposure stations are used in the printer, one for the computer-generated variable information, and the other for the fixed forms overlay. By necessity, to prevent interference between the two exposures, the information is carried in the exposed areas of the photoconductor and a reversal (exposed area) development is used. In the forms overlay station a xenon flash lamp exposes the photoconductor with a spectrally distributed light through a negative mask. The computer-generated information is applied to the photoconductor by line scanning a modulated heliumneon laser beam with a nominal exposure of about $5.5 \,\mu\text{J/cm}^2$.

A model for the internal and external photoconductor currents and their characteristics in time was developed to simulate the photoconductor response to charging and discharging steps in the printer and to define the requirements for the charging and exposure units. In the simulation a unit area of the photoconductor was considered to have a capacitance $C_{\rm p}$, a dark current $j_{\rm d}$, and a photocurrent $j_{\rm p}$, under illumination. With the photoconductor charged by an external current j from a corona, the capacitor charging current $j_{\rm c}$ is given by

$$j_{\rm c} = j - j_{\rm p} - j_{\rm d},\tag{1}$$

and the potential on the photoconductor by

$$V_{\rm p} = -\int \frac{\dot{J}_{\rm c}}{C_{\rm p}} dt. \tag{2}$$

The dark current was modeled by the equation

$$j_{d} = -V_{p} \{ \beta + \alpha [(1 - \phi)[jdt - [j_{d}dt]] \},$$
 (3)

where β , α and ϕ were constants determined experimentally. The dark current model used in the simulation was based both on experimental results and on theoretical considerations. The dark current is a complex time-de-

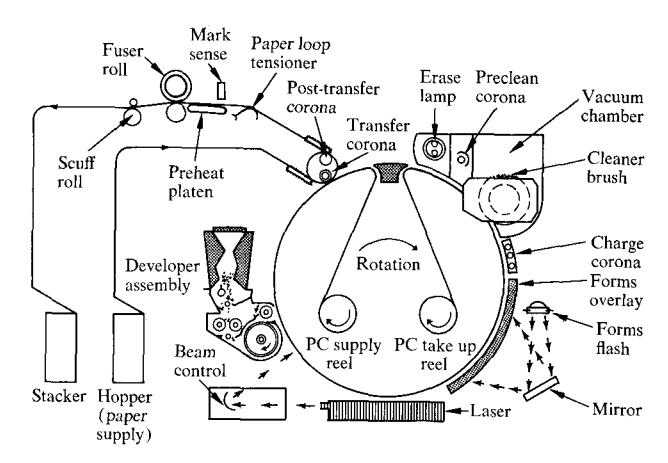


Figure 1 Configuration of the electrophotographic printing process.

pendent function of the potential across the photoconductor. Experimental observations made with the organic photoconductor indicate that current is high for a short interval after charging, but decreases considerably after an initial period of relaxation. The initial high current is dependent on the charging rate. Equation (3) describes these experimental observations. The equation consists of two terms, an ohmic term, βV_n , which becomes effective only some time after charging; and the "relaxation" term describing the initially high dark currents. The relaxation current depends on the net charge deposited on the photoconductor, $[jdt - [j_d dt], and it continues]$ until only a fraction of the charges ϕ is retained on the photoconductor. The rate of this relaxation current is given by α . The values for the constants used in simulation were: $\alpha = 1 \times 10^{-4} \text{ V}^{-1} \text{ s}^{-1}$, $\beta = 5 \times 10^{-11} \text{ A cm}^{-2} \text{ V}^{-1}$, and $\phi = 0.65$.

The photoinduced current density j_p was calculated from an equation based on the Li and Regensburger [6] derivation

$$j_{p} = K_{1} I V_{p} \left[1 - \exp\left(\frac{-K_{3}}{V_{p}}\right) \right] \exp\left(\frac{-K_{2}}{V_{p}}\right), \tag{4}$$

where I is the exposure intensity in μ W/cm². The constants were experimentally determined to fit the data for the organic photoconductor; they were: $K_1 = 4 \times 10^{-11}$ $(\Omega - \mu$ W)⁻¹, $K_2 = 25$ V, and $K_3 = 1.1 \times 10^3$ V.

Similarly, the mathematical model for the corona current j was based on experimental measurements. Two types of corona current measurements have been used in practice. In the first type of measurement a metal plate was placed under the corona, and the current to the plate was measured as a function of plate potential, giving a measure of the total current over the width of the corona. The distribution of the corona current was measured as a

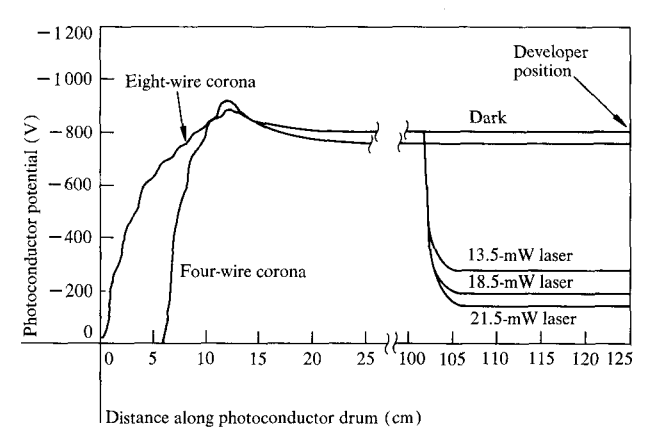


Figure 2 Simulation results for photoconductor potentials in two screened corona units, using four and eight corona wires and several different laser exposures.

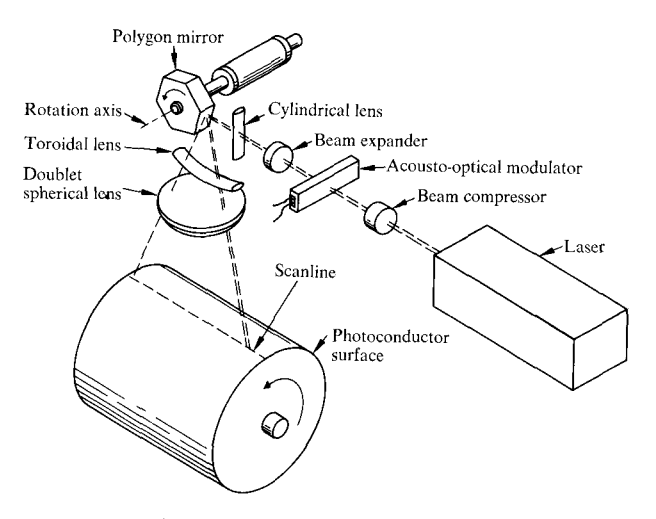


Figure 3 Optical path in the laser exposure system.

current to a narrow strip of conductor at ground potential placed lengthwise under the corona, and scanned across the width of the corona.

In simulations the instantaneous corona current was expressed as the product of the normalized distribution function and the total current as a function of the plate potential.

The analytic model presented in Eqs. (1) through (4) was used to predict photoconductor charge and discharge potentials and their variation in time for various charge corona configurations, laser and forms flash exposure levels and physical locations of the charge, discharge and development stations around the photoconductor drum. For a process speed of about 80 cm/s, Fig. 2 gives an example of the simulation results for two screen controlled corona units using four and eight corona wires and laser exposures of 13.5, 18.5, and 21.5 mW beam power. The

figure demonstrates a reduction in dark decay with a slower charging rate as accomplished with increasing numbers of corona elements. It also allows prediction of the contrast potential between exposed and unexposed areas of the photoconductor at the developer position and its variation due to laser power tolerances, as expected because of laser life and modulator efficiency changes.

The photoconductor is restored for the next cycle by exposing the total surface with a fluorescent erase lamp, neutralizing the remaining toner particles with a single-wire corona unit, and finally cleaning the photoconductor with a rotating brush and vacuum.

Laser exposure

The principal exposure of the photoconductor is performed by a scanning laser beam. A schematic of the laser exposure system is shown in Fig. 3. Intensity modulation of the laser light is accomplished by means of an electroacoustical modulator. A rotating mirror is used to provide line-scanning beam deflection. Even if the sensitivity of the photoconductor at a wavelength of 632.8 nm is only about 50 percent of the maximum, a helium-neon laser is used because of its power, life and stability characteristics.

The laser beam, with a nominal spot size of 0.4 mm at 10 percent of its Gaussian distribution, is operated at a scanning velocity of 1.88×10^5 cm/s on the photoconductor surface. With the nominal process speed of 80 cm/s and a flyback time of 10 percent, the scan resolution is 144 lines per inch. The laser modulator switching time of 75 ns allows a resolution in scan direction of 180 lines per inch. The horizontal line exposure intensity is obtained by convoluting spot size and slope with the scanning speed. Vertical intensity involves, in addition, convolution with the rise and fall times of the laser modulator. The convoluted exposures for horizontal and vertical lines are shown in Fig. 4.

Development

The development system had to be designed to produce consistently acceptable print quality, as measured by subjective visual and objective machine readable standards independent of the amount of information printed on a single page. In addition, the developer had to handle the photoconductor potentials and their variability due to photoconductor and exposure parameter changes over the component life. These have been estimated to be about -700 ± 75 V for the dark potential and -225 ± 75 V for the exposed potential.

The printer uses a parallel flow, dry toner, magnetic brush developer, as shown in Fig. 1. The magnetic brush technology was selected because of its superior ability to present charged toner to the electrostatic image within a small active development zone. The active development zone has been reduced and the replacement rate increased as far as is reasonable to minimize print reflectance variations in a print line caused by toner requirements of neighboring print lines.

In the developer a load of approximately 9 kg of carrier material is mixed with toner to about one hundredth of the carrier weight by the mechanical action of a pair of augers. The mechanical action serves also as the means to charge the toner with negative polarity through static electrification. Using specially prepared teflon-epoxy-coated magnetic beads with an average diameter of about 285 μ m as carrier and carbon black pigmented polystyrene-butylmethacrylate-based particles with an average particle size of 14.5 μ m as toner, the average toner charge at a nominal toner concentration of one percent by weight is 7.7×10^{-3} C/kg.

The charged toner on the magnetic carrier beads is transported into the development zone by a series of two rolls rotating in stationary magnetic fields. The magnetic field strength and rotational velocity were balanced with the roll surface roughness, the roll-to-roll spacing, and the magnetic-brush-to-photoconductor spacing to achieve a carrier velocity in the development zone of approximately two times the photoconductor velocity. The image development takes place when the electrostatic image forces exceed the force holding the toner to the carrier. The electrostatic charge on the toner is dependent on the amount of toner mixed with the carrier material. The toner concentration in the developer, therefore, is one of the main factors affecting image development. The toner concentration is adjusted by a feedback control loop sensing the reflectance of the output print. The toner control loop is discussed later in the section covering print reflectance control.

Image transfer

The developed image is transferred from the photoconductor to paper by applying an electrostatic charge sufficient to exceed the forces holding the toner to the photoconductor.

The transfer station has been designed for maximum transfer efficiency in a system with paperline start-stop capability between adjacent pages. The total active transfer zone allocated by paperline acceleration and deceleration demands [3] was found to be less than 12.7 mm. Since transfer efficiency is a function of applied charge, time, and mechanical contact, the system has been designed for maximum transfer corona current density, limited only by electrostatic discharge breakdown. A charge of about 4.2×10^{-8} C/cm² is applied to the back side of paper by a single-wire corona in a current-controlling high potential tube.

Static electrification of a moving paperline is a common problem in the paper industry and had to be considered

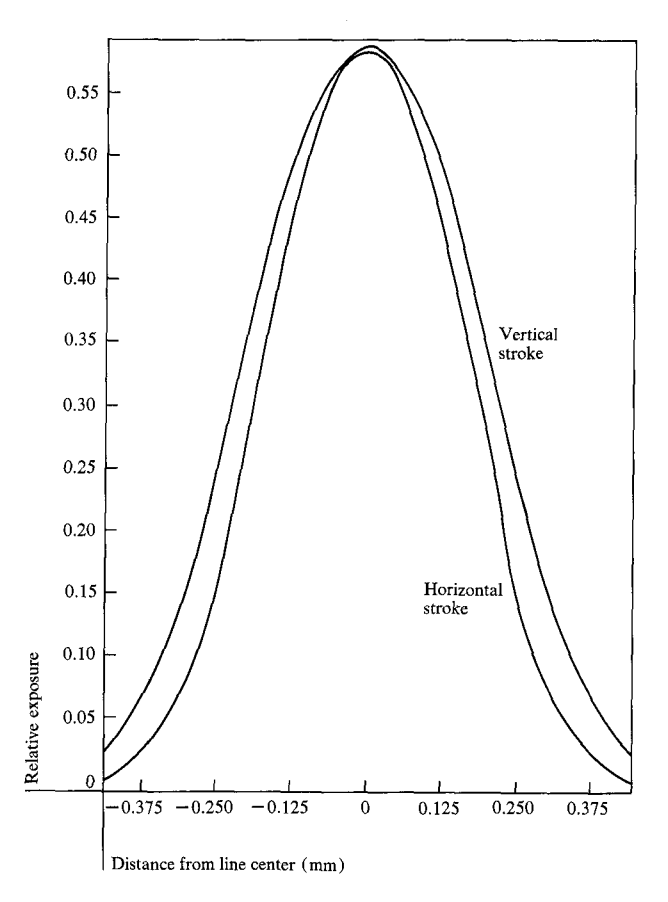


Figure 4 Convoluted laser exposure distributions for horizontal and vertical lines.

also in the printer design, especially in the transfer station, where uncontrolled paperline static charge can potentially destroy the image. A field is generated by charging the back side of the paper to the opposite polarity of the toner charge by means of a transfer corona. Depending on the electrical characteristics of the paper used and the electrical characteristics of the paper support structure, the charge on the paper will be the source of electrostatic forces. The electrostatically charged paper will form with the nearest groundplane or the supporting paperline structure a capacitor defining a field and electrostatic forces acting on the toner particles. At any transition in the paperline support between the transfer and fuser stations, a change in the capacitance is unavoidable. The originally normal electrical field with respect to paper could develop a parallel component. If the ratio of the normal to parallel field components exceeds the adherence of toner to paper, the toner will move, destroying the image information. This effect can significantly influence image quality.

In the printer this problem is controlled by neutralizing the paper charge with a post-transfer corona (see Fig. 1) and by a dielectric paperline support between the

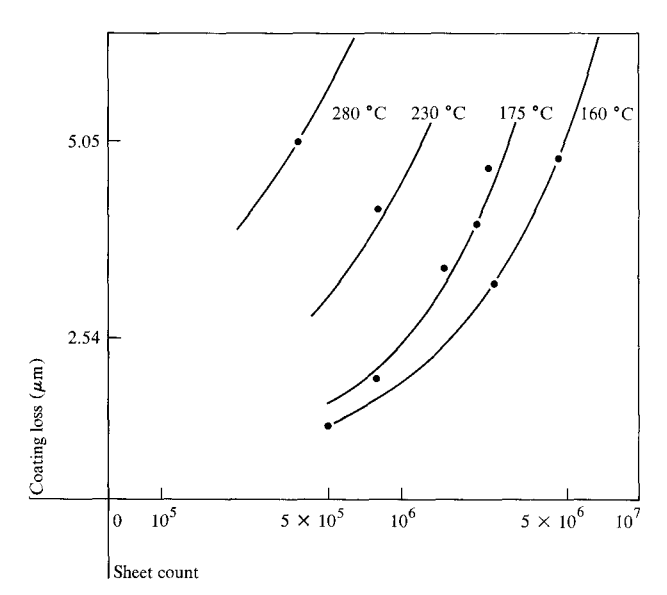


Figure 5 Hot roll coating loss as a function of roll life for various operating temperatures.

transfer and post-transfer coronas. The dielectric material chosen had to satisfy the following requirements: a) the material could not interact with the moving paperline in such a way that it could cause static electrification opposite to the paper charge under any environmental conditions; b) the material could not develop a surface charge of any polarity sufficient to create electrical fields able to move toner on or from the paper; and c) the material had to be of mechanical stability sufficient to sustain its shape within close tolerances while being worn by about 4000 miles of potentially highly abrasive paper running at high speed.

Fusing

After transfer the toned image is loosely held to the paper by electrostatic and mechanical forces. Permanent fusing of the toner onto the paper is accomplished at the fuser station with the application of heat and pressure. The fuser station (Fig. 1) uses a preheat platen to increase the paper temperature sufficiently to allow high speed hot roll fusing at moderate hot roll temperatures and pressures to obtain maximum safety and component life.

Thermomechanical considerations of polymers have been the prime factors in the fuser system design. Fusing is accomplished by increasing paper and toner temperatures beyond the melting point of toner while simultaneously applying pressure. The required temperature of 120°C to 165°C is obtained by preheating the paper with a platen and completing the fusing effort between a pair of polymer-coated rolls. The hot roll-backup roll combination serves, in addition, as a paper steering mechanism through the application of differential pressures at

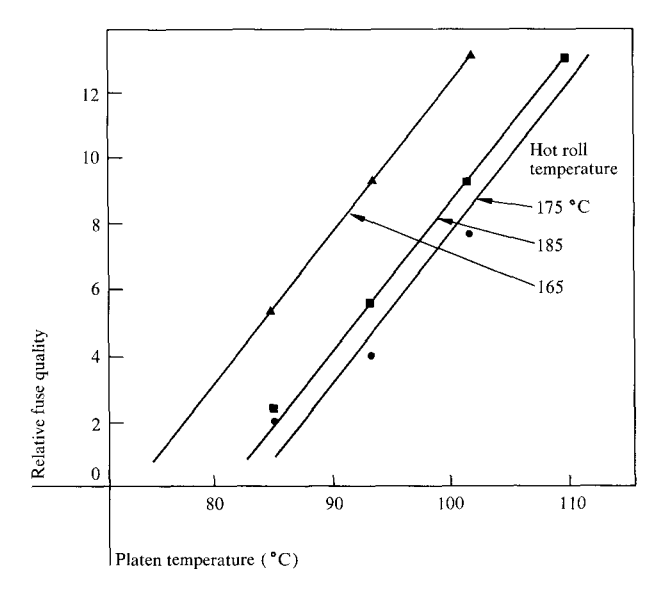


Figure 6 Effects of hot roll and platen temperatures on fuse quality.

the ends of the deformable backup roll. The roll deformations result in differential velocities at the surface layer of the molded backup roll, causing the desired steering effect.

Both the hot roll and the backup roll are limited in their life performances by loss of material caused by interaction with the paperline under the influence of elevated temperatures. The relationship between material loss of the hot roll and copy count for various operating temperatures is shown in Fig. 5.

The relative effect of hot roll and preheat platen temperatures for the same fuse quality is shown in Fig. 6. The increased life performance at lower hot roll temperatures provides the justification for the otherwise ineffective preheat platen. The hot roll and preheat platen temperatures were chosen to balance the life performance of the fusing system with its effectiveness. Details of the fuser design are given by Brooms [4].

Print density control

To achieve consistent print quality the printer is equipped with a print reflectance sensor that controls the toner feed rate. Since the print reflectance depends on various electrostatic and mechanical parameters in the printing subsystem, the toner control loop has to be capable of compensating for all expected parameter variations. One of the most important parameters is the charge on the toner particles in the mix of toner and carrier. The average charge per gram of toner is a function of toner concentration in the developer mix, as shown in Fig. 7. The charge-to-mass ratio decreases significantly with increased life of the carrier material because of a loss of charging ability in

the carrier. The decrease in charging ability in the carrier is caused by the gradual buildup of a permanent toner layer on the carrier beads, blocking a portion of the carrier surface. To obtain consistent print density over the changes in toner charge, the printer has an independent toner feed control that senses the print reflectance on the paper through a control mark. When the output print reflectance sensor indicates a print density lower than desired, the control loop will increase the feed rate. The additional toner will result in an increase of toner concentration in the mix of toner and carrier, resulting in an increase in print density. When the desired print density is achieved, the toner feed rate will be decreased to a lower value consistent with the amount of print generated. The toner loop compensates also for other variations in the electrophotographic process.

Summary

The electrophotographic process has been developed around the organic photoconductor material that has proved its function in the IBM Copier I and Copier II products. An eight-wire charge corona was developed to charge the photoconductor reliably to the desired dark potential and to minimize dark decay between the charging, exposure, and development stations. Helium-neon laser technology has been applied for the exposure of computer-generated information, because of its known reliability as a stable continuous light source of sufficient intensity and its applicability to high speed modulation and deflection. Magnetic brush development has been selected because of its ability to deliver charged toner to the electrostatic image at sufficiently high rates. The combination of a hot roll fuser and a preheat platen has been developed for the fusing station, in order to obtain high fuse quality at acceptable power consumption and adequate fuser hot roll life. A toner control system based on monitoring output print density has been implemented to assure consistent print quality independent of the changes in carrier and other electrophotographic parameters.

Acknowledgments

The work described above reflects important contributions by many individuals. It is not possible to list all of them here, but special acknowledgment must go to R. A. Jensen, who has also been involved extensively in the process development.

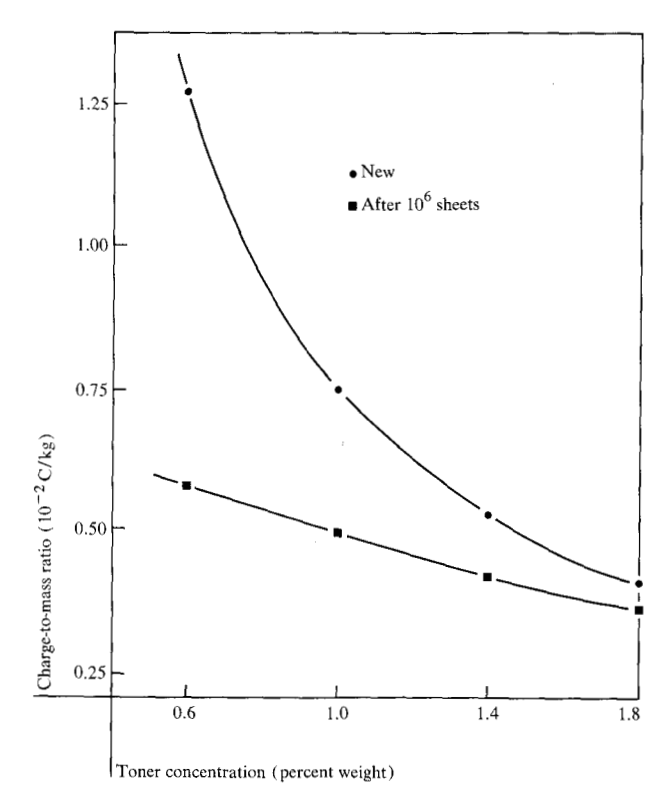


Figure 7 Relation of toner charge-to-mass ratio to toner concentration for new and used carriers.

References

- 1. R. G. Svendsen, *IBM J. Res. Develop.* 22, 13 (1978, this issue).
- 2. G. I. Findley, D. P. Leabo, and A. C. Slutman, *IBM J. Res. Develop.* 22, 2 (1978, this issue).
- 3. T. J. Cameron and M. H. Dost, *IBM J. Res. Develop.* **22**, 19 (1978, this issue).
- K. D. Brooms, IBM J. Res. Develop. 22, 26 (1978, this issue).
- 5. R. M. Schaffert, IBM J. Res. Develop. 15, 75 (1971).
- H. T. Li and P. J. Regensburger, J. Appl. Phys. 34, 1730 (1963).

Received May 24, 1977

The authors are located at the IBM General Products Division laboratory, 5600 Cottle Road, San Jose, California 95193.